Molecular Beam Epitaxial Growth of Zinc-Blende FeN(111) on Wurtzite GaN(0001)

Wenzhi Lin, Jeongihm Pak, David C. Ingram, and Arthur R. Smith*

Nanoscale and Quantum Phenomena Institute,

Department of Physics and Astronomy,

Ohio University, Athens, OH 45701, USA

Abstract

We report a study of the growth of iron nitride on gallium nitride using molecular beam epitaxy with Fe e-beam evaporation and rf N-plasma growth. Thin iron nitride layers of thickness about 16 nm were grown and monitored *in-situ* using reflection high energy electron diffraction. The samples following growth were analyzed *ex-situ* using a variety of techniques including x-ray diffraction, Rutherford Backscattering, and atomic force microscopy. By monitoring the structure, morphology, and lattice constant evolution of the iron nitride film, the crystal phase and orientation with respect to the GaN substrate are deduced; and from RBS data, the stoichiometry is obtained. The growth is discussed in terms of a 2-D to 3-D growth mode transition, and a critical thickness is estimated.

Keywords: Nitride materials; Crystal growth; Crystal structure; X-ray diffraction

* e-mail: smitha2@ohio.edu

INTRODUCTION

Iron nitrides, having various complex phases such as $Fe_{16}N_2$,Fe_8N, Fe_4N, Fe_3N_2, Fe_2N, and FeN, are attractive for their high magnetic moments [1], corrosion and oxidation resistance [2], and many other attractive properties. Motivated by the potential attractive properties, there have been many attempts to achieve Fe-N films of various composition, and using various growth methods including sputtering[3–9], nitriding [10–14], ion implantation[15–18], and molecular beam epitaxy (MBE) [19–23].

Unfortunately, it is difficult to prepare Fe-N films having a single phase, which increases the difficulty of analyzing the properties of the separate phases. It is thus important and useful to explore growth of high quality single phase epitaxial Fe-N films [24]. While the more Fe-rich phases are expected, and have been found, to be magnetic, the phases closer to 1:1 stoichiometry are also very interesting for potential applications.

While zinc-blende FeN has not been reported to have high magnetic moment, it is possible that by growing on different types of substrates (forming strained layers), or by alloying with other nitrides, the material could become magnetic. For example, a theoretical paper has shown the existence of metastable magnetic states in zinc-blende FeN for unit cell volumes larger than the equilibrium value[25]. Therefore it is interesting to explore the growth of FeN in the zinc-blende phase.

In previous studies, Fe-N films have been grown on a wide range of conventional cubic structure substrates, such as MgO[5, 15], GaAs[19], InGaAs [20, 22], NaCl [7, 18], and Ge [26], but not hexagonal (wurtzite) GaN, a fast-developing semiconductor material with important technological applications. *w*-GaN is an attractive substrate due to its wide band-gap (3.4 eV), ultra-violet light emitting characteristics, high hardness, and high-temperature stability.

It might be assumed to be difficult to combine a cubic material film with a hexagonal material substrate. However, as shown recently in our group [27], in some cases cubic structure films can match very well with hexagonal substrates, given a particular growth orientation.

In this paper, we report successful epitaxial growth of high quality zinc-blende FeN on wurtzite GaN(0001), by employing e-beam evaporation in an ultra-high vacuum MBE chamber. The FeN films have a well-oriented epitaxial relationship with the substrate and grow

smoothly for the first few monolayers.

EXPERIMENTAL

The experiments were performed in a custom-designed ultrahigh vacuum (UHV) MBE system with base pressure of low 10^{-10} Torr. Films were grown using an Fe e-beam evaporator and a radio-frequency (rf) nitrogen (N_2) plasma source. The Fe flux was calibrated using a quartz crystal thickness monitor. The N flux was set by the N_2 flow rate and plasma source power.

The substrates used were wurtzite GaN(0001) grown on sapphire(0001) using metal-organic chemical vapor deposition by a commercial vendor. Substrate surfaces were first cleaned with acetone and isopropyl alcohol, then loaded into the MBE chamber and either heated up to $\sim$ 650-700 °C for 5 min, or else refreshed with a new layer of GaN by MBE growth.

During growth, reflection high energy electron diffraction (RHEED) using 20 keV electrons was used *in-situ* to monitor the surface structure and the in-plane lattice parameter. After removal of the grown sample from the chamber, *ex-situ* x-ray diffraction (XRD) using Cu K_α x-rays, was used to determine the crystal structure and out-of-plane lattice parameter. In addition, *ex-situ* Rutherford Backscattering (RBS), using incident He^+ ions of energy 5.6 or 2.2 MeV, was also carried out to further investigate the crystal structure. Atomic force microscopy (AFM) was used to determine the surface morphology.

For the FeN film growth reported here, the substrate temperature was set to $\sim$ 210 °C, the Fe flux was set to $\sim 2.3 \times 10^{13}/\mathrm{cm}^2$ s, and the growth chamber pressure was set to $\sim 9.3 \times 10^{-6}$ Torr with the rf N plasma forward power set to 500 W. The total growth time for the FeN layers discussed here was about 2 h. For the growth conditions used, the rate of FeN growth was $\sim$ 155 Å/2hr ($\pm$ 4%) based on the thickness (for 2 hour growth) estimated from RBS data which yields the sample total number of Fe atoms per unit area. Comparing to the growth rate expected based on the Fe flux rate measured, we find an effective Fe sticking coefficient S during FeN growth of about 0.48.

RESULTS AND DISCUSSION

RHEED Evolution

Shown in Fig. 1(a) is the RHEED pattern of a wurtzite GaN(0001) substrate surface along $\langle 11\bar{2}0 \rangle$ taken before the start of FeN growth. The streaky pattern indicates a smooth starting substrate surface. Shown in Figures 1(b) - 1(f) are RHEED pattern clips extracted from a 10 minute movie that captured the very early stage of an iron nitride film growth on GaN. Each clip shows that the growth orientation of the FeN film conforms to that of the substrate. Later, we discuss the particular orientation and further deduce the crystal structure.

Figure 1(b) was captured at 30 s after the growth started, corresponding to about 1/4 monolayer (ML) of deposition. The slightly less streaky RHEED pattern suggests an initial 2-dimensional islanding growth mode. In Fig. 1(c), captured at 60 s or $\sim 1/2$ ML deposition, the RHEED pattern continues to be similar. At 120 s corresponding to one ML deposition, we see that the pattern is more streaky, as seen in Fig. 1(d); this suggests that the first ML is very smooth. This could be due to the merging of islands to form a complete layer.

After 120 s, the RHEED pattern becomes increasingly less streaky. This can be seen at 240 s (2 ML) and 360 s (3 ML), as seen in Figs. 1(e) and 1(f). It is consistent with a transition from a two-dimensional to three-dimensional growth. The initial stage of the growth was followed up to 600 s, about 5 ML, in which this trend continued. The roughening behavior seen between 120 s and beyond is consistent with growth past a critical thickness involving strain relaxation via the formation of three-dimensional islands, defects, and dislocations.

Lattice Spacing Evolution

The whole growth evolution for the first 5 ML appears to be consistent with a two-dimensional followed by three-dimensional mode, or the well-known Stranski-Krastanov (S-K) growth mode [28]. To further investigate this initial growth stage, we also measured, using the RHEED reciprocal streak spacing, the lattice spacing versus initial growth thickness for the duration of the 600 s period. This data is plotted in Fig. 2, which shows the atomic row spacing as a function of time.

We see that during the first two ML (up to about 240 s) there are some variations or oscillations in the lattice spacing, with an average trend of increasing, starting from the initial GaN inter-row spacing (2.76 Å). At about 2 ML and thicker, the trend is predominantly that the spacing steadily decreases. Below, we offer some possible explanations for the early variations in lattice spacing; such variations at the initial stage of growth differ somewhat from the classical pseudomorphic growth model, in which in the simplest case one expects a constant value up to the critical thickness. Nevertheless, after about 2 ML, the steady decreasing lattice parameter trend is quite consistent with well-known strain relaxation behavior. This is therefore suggestive of a critical thickness of about 2 ML ($\sim$ 5 Å).

Crystal Structure Evolution at the Early Stage of Growth

Going back to Fig. 1, we notice an additional feature in the data not yet discussed. As the growing FeN film is not perfectly atomically flat, we observe modulations along the streak direction which are due to sampling of several ML's deep into the surface (this can be due to few-ML height islands on the surface). As seen in Fig. 1(b), the top 3 highest intensity points are lined up horizontally, the same as for the GaN surface [Fig. 1(a)]. However, clearly visible by 60 s and always after that, we observe a trend of these spots becoming increasingly non-collinear (not lined up along the horizontal).

This shift in the spot-pattern is consistent with a trend from wurtzite structure toward face-centered cubic structure (either rocksalt or zincblende) [29]. Such a structural transition is expected, since the structure of FeN is reported to be face-centered cubic, either rock-salt or zinc-blende [30]. The fact that we see evidence of a structural transition at such an early stage of the growth (well before the critical thickness is reached) may partly explain the lattice spacing variations also seen during this early stage. It is also possible that there could be some degree of intermixing of Ga and Fe at the interface which could also affect the lattice spacing in a complex way. Further experiments are underway to explore the latter possibility.

FeN on GaN Growth Beyond the Critical Thickness

For the remainder, we focus on the growth above the critical thickness (about 2 ML). As seen in Fig. 2, the lattice spacing above two ML steadily decreases, consistent with a relaxation phase. While the continuous RHEED acquisition ended at 600 s (about 5 ML), individual RHEED patterns were acquired up to the final growth thickness (63 ML) for several different samples.

For the data shown in Fig. 2, the *in-plane* lattice spacing shows a change of already -0.05 Å starting from 240 s (near h_c = 2 ML) up to 600 s (5 ML); given that the additional lattice spacing change from that point (5 ML) up to the relaxed FeN thickness is expected to be -0.075 Å (= 2.66 - 2.735 Å), we estimate, using a linear extrapolation model, that the film surface layer will reach the fully relaxed FeN lattice constant at $\sim$ 10 ML total film thickness (= 8 ML past h_c). Out of a total film thickness of 155 Å (63 ML), we expect therefore about 84 % of the film to be fully relaxed.

Shown in Fig. 3(a) is the RHEED pattern along the same direction ($[\bar{1}10]$) as in Figs. 1(a-f), here taken at the end of a growth ($\sim$ 155 Å). Fig. 3(b) shows the RHEED pattern taken along $\langle 11\bar{2} \rangle$. Neither RHEED pattern is streaky, suggesting a 3-D mode at the final stage of growth.

We also see [Fig 3(a)] that the spot pattern has fully evolved to that of fcc. For comparison, the inset to Fig. 3(a) shows a reciprocal space map calculated from a superposition of structure factors for two inequivalent [111]-oriented fcc grains. The two inequivalent grains are rotated by 180° with respect to each other; if there was only one type of grain, the RHEED spot pattern would be left-right asymmetrical.[29].

A bimodal distribution of grains is understandable, based on the fact that since fcc along [111] has 3-fold symmetry, it will tend to follow epitaxially upon a 3-fold symmetric substrate template. And, although the wurtzite structure has 3-fold bulk crystal symmetry about [0001], the bond directions rotate by 180° upon crossing any single (or odd multiple of single) monolayer step of the [0001] wurtzite surface, leading to A-type and B-type GaN steps and terraces. Therefore, since we expect as many A-type as B-type terraces, we can expect that both types of FeN grains will nucleate, consistent with the final RHEED pattern.

The in-plane lattice constants for several different FeN films at the end of the 155 Å growth were measured from RHEED patterns such as shown in Fig. 3. Thus the final layer

in-plane spacing was found in the range 2.63 - 2.66 Å or a = 4.29 - 4.34 Å.

Epitaxial Orientation with GaN Substrate

The XRD pattern for a FeN film grown for 2 hours on GaN is shown in Fig. 4. The spectrum was calibrated using the wurtzite GaN peak as the reference peak. It should therefore locate at 34.60 degrees assuming c_{GaN} = 5.185 Å and a Cu K_α mean wavelength = 1.5418 Å. Besides the large GaN peak, there are two other significant peaks at 36.45 and 77.25 degrees. These peaks correspond to the FeN film; their small intensities are due to the very small FeN film thickness (about 155 Å) compared to the substrate.

Assuming the two small peaks correspond to the first and second order for the FeN (111 and 222 peaks), we calculate an FeN film average interplanar (c-direction) spacing of 4.27 Å. This value is in fairly good agreement with the lattice constant reported for zinc-blende type γ ”-FeN, 4.33 Å [30].

As shown in Fig. 2, the in-plane lattice constant is stretched in the strained layer. By the volume conservation principle, the out-of-plane lattice constant is therefore expected to be contracted in the strained layer, compared to a relaxed layer. Thus it is reasonable that our measured XRD (*out-of-plane*) lattice constant (a=4.27 Å) should be slightly smaller than the true relaxed lattice constant, since it is the average of both strained and relaxed layers. In fact, it is slightly smaller than our *in-plane* lattice constant (a = 4.29 Å- 4.34 Å) at the end of growth measured by RHEED. Note that our RHEED value is very consistent with the reported zinc-blende value of 4.33 Å.[30]

The RHEED and XRD data are therefore quite consistent with each other, and both support the conclusion that the FeN film has a zinc-blende crystal structure with (111) orientation. Furthermore, our measured FeN lattice constant is certainly inconsistent with that reported for the rock-salt structure (4.50 Å)[30]. Thus, for our growth conditions, we find the epitaxial orientation with the GaN substrate to be $[111]_{ZB-FeN} \parallel [0001]_{w-GaN}$.

Using RBS data, our FeN film stoichiometry was measured, and the result was found to be iron fraction F_{Fe} = 55-58% and corresponding N fraction F_N = 45-42%. This result is also consistent with previous experiments which found N fractions less than 50%[30]. Since our lattice constant values do not suggest metal interstitials, the RBS data therefore indicates N vacancies for our sample. N vacancies are in fact very common for transition metal nitrides,

including ScN and MnN,[31, 32] which we have previously investigated. Therefore, we infer that the FeN film has a composition ratio of Fe:N in the range 1.0:0.82 - 1.0:0.72.

Now we discuss the in-plane orientation of the FeN film with respect to the GaN substrate. The FeN crystal vector directions for the RHEED patterns (shown for example in Figs. 3(a) and 3(b)) correspond to the substrate GaN $\langle 11\bar{2}0\rangle$ and $\langle \bar{1}100\rangle$, respectively. Thus, we also see that the azimuthal (in-plane) orientation of the film is lined up with that of the substrate, and there is no rotation of the film with respect to the substrate. Thus we have the in-plane orientations $\langle \bar{1}10\rangle_{FeN} \parallel \langle 11\bar{2}0\rangle_{GaN}$ and $\langle 11\bar{2}\rangle \parallel \langle 1\bar{1}00\rangle$.

In fact, this orientation was assumed already in displaying the calibration for Fig. 2 and the discussion of the lattice parameters of the FeN films, in which the inter-atomic spacing of Ga atoms, being 3.189 Å, leads to the inter-row spacing of the $\langle 11\bar{2}0\rangle$ direction equal to 2.76 Å. This spacing compares to the measured values for the relaxed FeN film of 2.63 - 2.66 Å, corresponding to an Fe-Fe inter-atomic spacing of 3.04 - 3.07 Å. The in-plane mismatch between the film and the substrate is therefore about -4.2 %.

Film Topography and Epitaxial Growth Model

As seen in Fig. 5, the AFM image of the as-grown FeN film shows an array of uniformly distributed 3-D islands having lateral diameters of $\sim$ 84 nm (valley-to-valley). These 3-D islands are spaced quite closely together, showing that they have merged to form a nearly continuous thin film. Analysis of the image shows that the root-mean-square(rms) roughness is 1.44 nm, but line profile measurements find islands having heights in the range $\sim$ 1 - 8 nm. The larger island diameters (widths) compared to the much smaller island heights (width:height ratio = 10 - 84) shows that the surface, while not atomically flat, is still relatively smooth.

In Fig. 6, we show the structural model of the FeN (111) film growth on Ga-polar *w*-GaN(0001). The upward directions are [111] and [0001] for FeN and GaN, respectively. Their perpendicular out-of-plane directions are $\langle \bar{1}10\rangle$ for FeN and $\langle 11\bar{2}0\rangle$ for GaN. This model is based upon the conclusions drawn from the experimental data presented here. The film grows very smoothly with only small lattice spacing variations for the first about 2 ML, implying a strained initial layer. After this initial 2 ML, which corresponds to the critical thickness (about 5 Å), the film begins to relax during growth up to a layer thickness of at

least 10 ML = ∼ 25 Å. The relaxation process correlates with a change from 2-D to 3-D growth. Also, we observed that the crystal structure very quickly evolved from wurtzite to zinc-blende within as little as a few ML, and is fully evolved into zinc-blende by the end of the 155 Å growth.

CONCLUSIONS

We demonstrated the growth of (111)-oriented FeN thin layers on GaN(0001) using molecular beam epitaxy using e-beam evaporation of Fe in combination with rf N-plasma with N_2 as the source gas. The results are that the FeN growth is consistent with a 2-D to 3-D (S-K) growth mode. The 2-D mode portion of the growth extends to about 2 ML. After this, the film began to relax, and we estimate an additional 8 ML (at least) of growth before reaching the fully relaxed lattice constant. The relaxation process correlates with a roughening of the film surface. Also, even from the very early stage of growth, the RHEED pattern shows signs of conversion from wurtzite structure at the FeN/GaN interface to face-centered cubic structure. Careful analysis of the RHEED and XRD data leads to the conclusion that the grown film has zinc-blende structure with relaxed lattice constant a in the range 4.29 - 4.34 Å. Furthermore, the RBS data finds that the FeN stoichiometry is Fe:N = 55:45 (1.0:0.82) up to 58:42 (1.0:0.72); the data suggests the existence of N vacancies. The film is epitaxial with the substrate, and the epitaxial orientation was determined to be $[111]_{FeN} \parallel [0001]_{GaN}$ and $\langle\bar{1}10\rangle_{FeN} \parallel \langle 11\bar{2}0\rangle_{GaN}$ and $\langle 11\bar{2}\rangle_{FeN} \parallel \langle 1\bar{1}00\rangle_{GaN}$, with two types of [111]-oriented FeN grains, 180° apart from each other.

ACKNOWLEDGEMENTS

This work has been directly funded by the U.S. Department of Energy, Office of Basic Energy Sciences (Grant No. DE-FG02-06ER46317). The authors also thank Dr. Erdong Lu for useful discussions.

---

[1] T. K. Kim, M. Takahashi, Appl. Phys. Lett. 20 (1972) 492-494.

[2] S. F. Matar, G. Demazeau, B. Siberchicot, IEEE Transactions on Magnetics 26 (1990) 60-62.

[3] N. Heiman, N. S. Kazama, J. Appl. Phys. 52 (1981) 3562-3564.

[4] C. Gao, W. D. Doyle, M. Shamsuzzoha, J. Appl. Phys. 73 (1993) 6579-6581.

[5] M. Takahashi, H. Shoji, H. Takahashi, H. Nashi, T. Wakiyama, M. Doi and M. Matsui, J. Appl. Phys. 76 (1994) 6642-6647.

[6] S. R. Kappaganthu, Y. Sun, Surf. Coat. Technol. 167 (2003) 165-169.

[7] D. C. Sun, C. Lin, E. Y. Jiang, J. Phys.: Condens. Matter 7 (1995) 3667-3674.

[8] M. A. Brewer, K. M. Krishnan, J. Appl. Phys. 79 (1996) 5321-5323.

[9] D. C. Sun, E. Y. Jiang, D. Sun, Thin Solid Films, 298 (1997) 116-121.

[10] K. H. Jack, J. Alloys Compd. 222 (1995) 160-166.

[11] W. E. Wallace, M. Q. Huang, J. Appl. Phys. 76 (1994) 6648-6652.

[12] M. Q. Huang, W. E. Wallace, S. Simizu, A. T. Pedziwiatr, R. T. Obermyer, S. G. Sankar, J. Appl. Phys. 75 (1994) 6574-6576.

[13] X. Bao, R. M. Metzger, M. Carbucicchio, J. Appl. Phys. 75 (1994) 5870-5872.

[14] X. Bao, R. M. Metzger, W. D. Doyle, J. Appl. Phys. 73 (1993) 6734-6736.

[15] K. Nakajima, S. Okamoto, Appl. Phys. Lett. 54 (1989) 2536-2538.

[16] K. Nakajima, S. Okamoto, T. Okada, J. Appl. Phys. 65 (1989) 4357-4361.

[17] K. Nakajima, T. Yamashita, M. Takata, S. Okamoto, J. Appl. Phys. 70 (1991) 6033-6035.

[18] E. Leroy, C. Djega-Mariadassou, H. Bernas, O. Kaitasov, R. Krishnan, M. Tessier, Appl. Phys. Lett. 67 (1995) 560-562.

[19] M. Komuro, Y. Kozono, M. Hanazono, Y. Sugita, J. Appl. Phys. 67 (1990) 5126-5130.

[20] Y. Sugita, K. Mitsuoka, M. Komuro, H. Hoshiya, Y. Kozono, M. Hanazono, J. Appl. Phys. 70 (1991) 5977-5982.

[21] H. Takahashi, K. Mitsuoka, M. Komuro, Y. Sugita, J. Appl. Phys. 73 (1993) 6060-6062.

[22] Y. Sugita, H. Takahashi, M. Komuro, K. Mitsuoka, A. Sakuma, J. Appl. Phys. 76 (1994) 6637-6641.

[23] H. Takahashi, M. Igarashi, A. Sakuma, Y. Sugita, IEEE Trans. Magn. 36 (2000) 2921-2923.

[24] L. Rissanen, M. Neubauer, K. P. Lieb, P. Schaaf, J. Alloys Compd. 274 (1998) 74-82.

[25] Y. Kong, J. Phys.:Condens. Matter 12 (2000) 4161-4173.

[26] X. Ding, F. Zhang, J. Yan, H. Shen, X. Wang, X. Liu, D. Shen, J. Appl. Phys. 82 (1997) 5154-5158.

[27] E. Lu, D. C. Ingram, A. R. Smith, J. W. Knepper, F. Y. Yang, Phys. Rev. Lett. 97 (2006)

146101-1 - 146101-4.

[28] I. N. Stranski, Von L. Krastanow, Akad. Wiss. Lit. Mainz Math.-Natur. Kl. IIB 146 (1939) 797.

[29] C. Constantin, H. Al-Brithen, M. B. Haider, D. Ingram, A. R. Smith, Phys. Rev. B 70 (2004) 193309-1 - 193309-5.

[30] T. Hinomura, S. Nasu, Physica B 237-238 (1997) 557-558.

[31] H. A. H. Al-Brithen, E. M. Trifan, D. C. Ingram, A. R. Smith, and D. Gall, J. Crystal Growth 242 (2002) 345-354.

[32] H. Yang, H. Al-Brithen, A. R. Smith, E. Trifan, and D. C. Ingram, J. Appl. Phys. 91(3) (2002) 1053-1059.

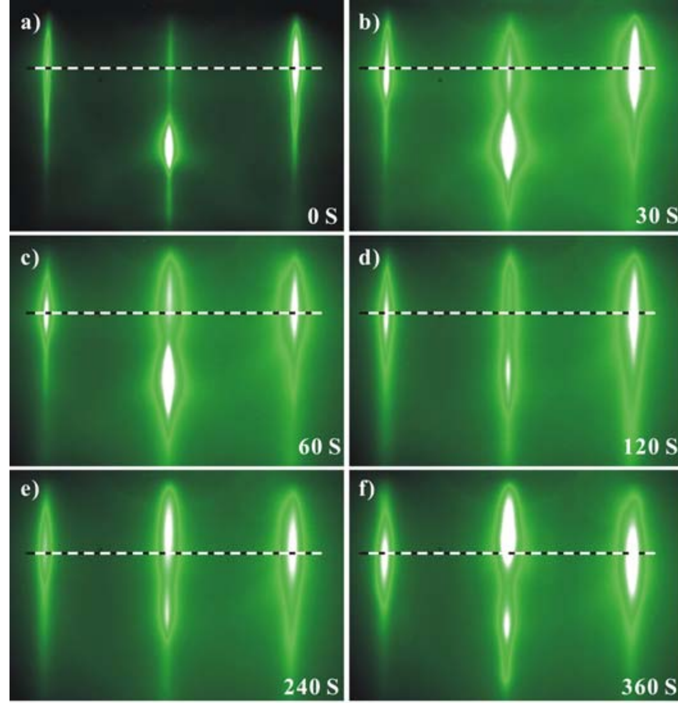

FIG. 1: RHEED patterns for w-GaN(0001) substrate and FeN thin film surface during growth. (a) GaN surface before FeN growth, along $\langle 11\bar{2}0\rangle$; (b-f) initial stages of FeN growth, along $\langle \bar{1}10\rangle$.

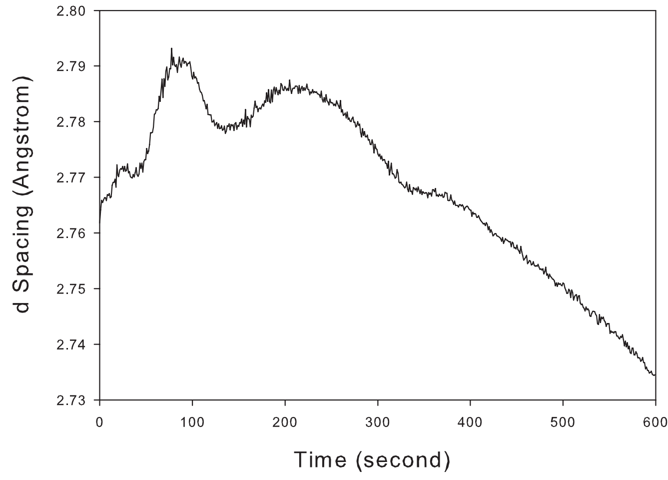

FIG. 2: In-plane inter-row spacing vesus time, measured for the $\langle\bar{1}10\rangle_{FeN} \parallel \langle 11\bar{2}0\rangle_{GaN}$ azimuth, and at the growth temperature.

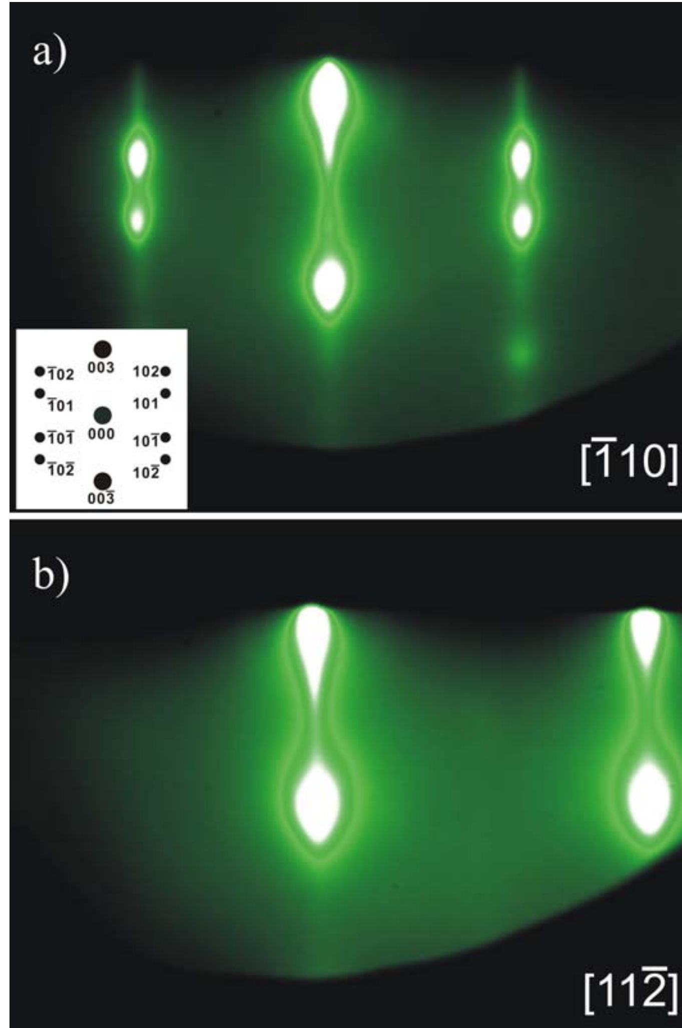

FIG. 3: RHEED patterns taken from the FeN layer after the growth. (a) [$\bar{1}10$] azimuth; inset is the corresponding reciprocal space map calculated for two inequivalent [111]-oriented fcc grains; (b) [$11\bar{2}$] azimuth. Both RHEED patterns were taken at the growth temperature.

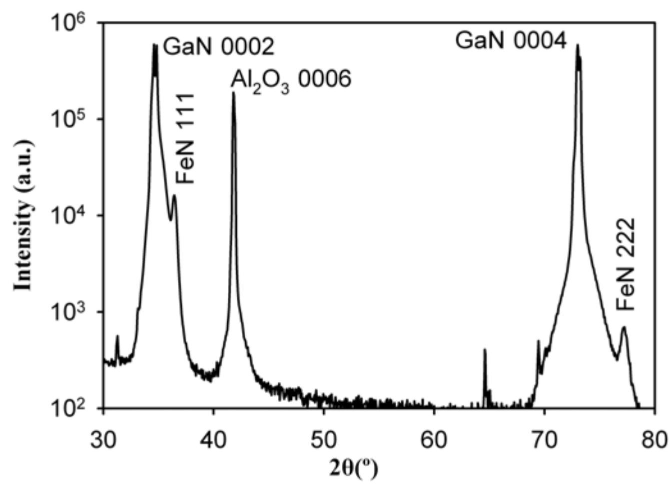

FIG. 4: XRD 2θ spectra of FeN sample grown on Ga-polar w-GaN(0001). Measurement was made at room temperature.

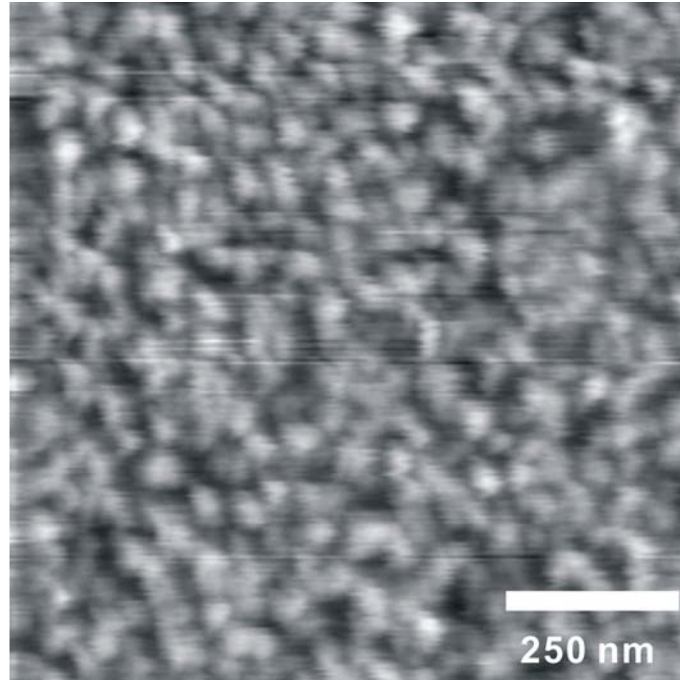

FIG. 5: AFM image of a FeN film after 2 hour growth. The peak-valley height for the whole image area is $\sim$ 10 nm, while the typical island height is 4-5 nm.

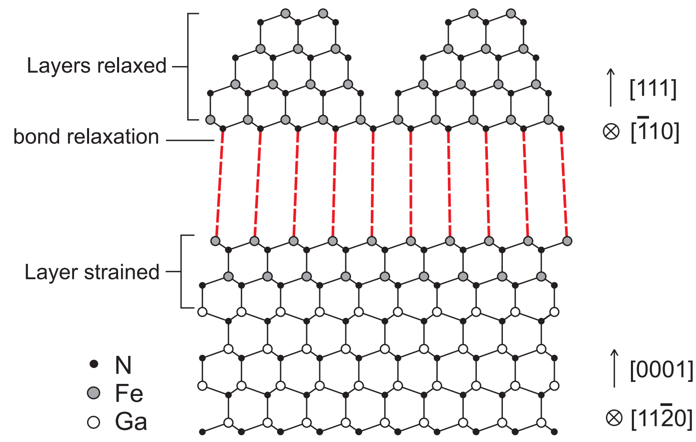

FIG. 6: Structural model of FeN(111)/GaN(0001) in side view showing epitaxial relationship of FeN(111) to Ga-polar w-GaN(0001). Topography suggested is only qualitative.